SPRAY COOLING APPLICATIONS FOR ALTERNATIVE ENERGY VEHICLES

BY

GEORGE POPOVIC

THESIS

Submitted in partial fulfillment of the requirements
for the degree of Master of Science in Mechanical Engineering
in the Graduate College of the
University of Illinois at Urbana-Champaign, 2021

Urbana, Illinois

Adviser:

Associate Professor Nenad Miljkovic

ABSTRACT

The number of electric and alternative fuel source vehicles has dramatically expanded in the last decade due to the proliferation of high energy dense batteries and lowering costs of hydrogen fuel vehicles. However, current generation heat exchangers take up more space in alternative fuel source vehicles than in traditional combustion vehicles due to the lower allowable temperatures of the battery or fuel source than the temperatures in a combustion engine. Large heat exchangers create a packaging problem for engineers, driving up the costs and reduce range due to the induced drag. Here we examine utilizing water to spray onto the heat exchangers to increase performance, allowing a decrease in surface area required for heat exchangers in alternative fuel source vehicles. The scalable and optimized superhydrophilic heat exchangers developed here at UIUC have the ability to increase the spray cooling system efficiency and decrease material usage and manufacturing costs.

TABLE OF CONTENTS

Nomenclature

CA	Contact angle	(°)
CHF	Critical Heat Flux	(W)
v_{air}	Airflow velocity	(m/s)
ΔP_{nozzle}	Pressure drop across the airflow nozzle	(Pa)
A_2	Outlet area of the airflow nozzle	(m^2)
A_1	Inlet area of the airflow nozzle	(m^2)
ρ_{air}	Density of air	(kg/m^3)
$T_{\text{air,inlet}}$	Temperature of the air entering the heat exchanger	(°C)
$T_{\text{air,outlet}}$	Temperature of the air exiting the heat exchanger	(°C)
$RH_{\text{air,inlet}}$	Relative humidity of the air entering the heat exchanger	(%)
$RH_{\text{air,outlet}}$	Relative humidity of the air exiting the heat exchanger	(%)
$T_{\text{TF,inlet}}$	Temperature of the fluid entering the heat exchanger	(°C)
$T_{\text{TF,outlet}}$	Temperature of the fluid exiting the heat exchanger	(°C)
$\dot{m}_{\text{TF}}$	Mass flowrate of the test section fluid	(kg/s)
ST	Spray temperature	(°C)
SP	Spray pressure	(PSI)

CHAPTER 1: INTRODUCTION

[1] [2] Heat dissipation and removal is the current bottleneck in power-dense high heat flux electronic environments which can cause high operating temperatures and lower product life cycles. Spray cooling has the potential to effectively cool the increasingly power-dense components being developed for use in the next-generation alternate fuel vehicles. Spray cooling systems that utilize rationally designed surfaces display significantly increased heat removal rates while utilizing smaller heat exchangers, thereby reducing the size-footprint of the system and decreasing the materials cost during manufacturing. Spray cooling systems are already being used in large-scale high heat-flux industrial systems such as the Cray X-1 supercomputer system [3], high power devices such as MOSFET's [4],and steel production [5]. Spray cooling is when liquid (in most applications water) is pressurized through a nozzle with a small diameter opening which results in a fine mist or spray of droplets which impinge upon a surface i.e. electronic component, heat exchanger, metals, etc. The droplets then spread on the surface forming a thin film, or evaporate, which results in large removal of heat. [6] Cader's study has shown that spray cooled server boards have exhibited significantly improved heat removal rates when compared to traditional air-cooled versions under identical power cycling conditions, where the diode temperatures on the spray cooled server boards were 33.3°C lower .[7] Cader et al. anticipate this reduction in die and junction temperature will allow for higher clock speeds of processors in the future. Sienski et al. showed the advantages of spray cooling as compared to forced air convection and forced water convection in the figure below. [8]

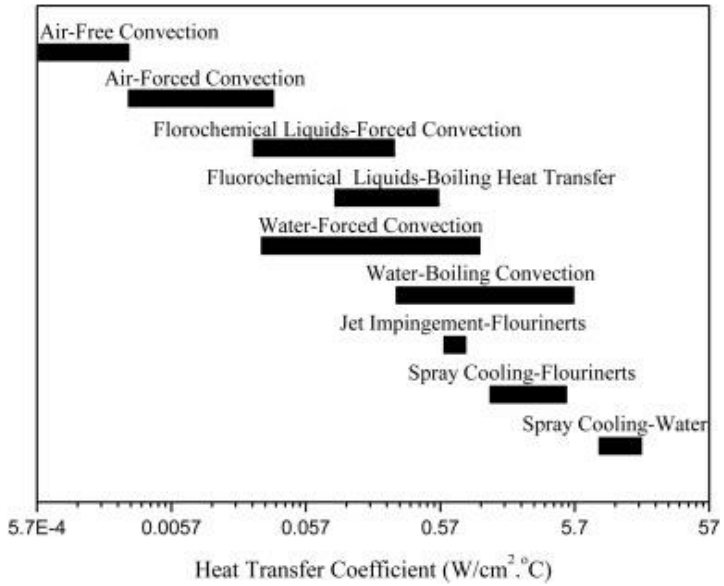

Fig. 1. Heat Transfer Coefficients (Figure adapted from reference [8] with permission)

Figure 2 shows how the heat flux changes according to the wall temperature in a regular spray cooling application.[9]

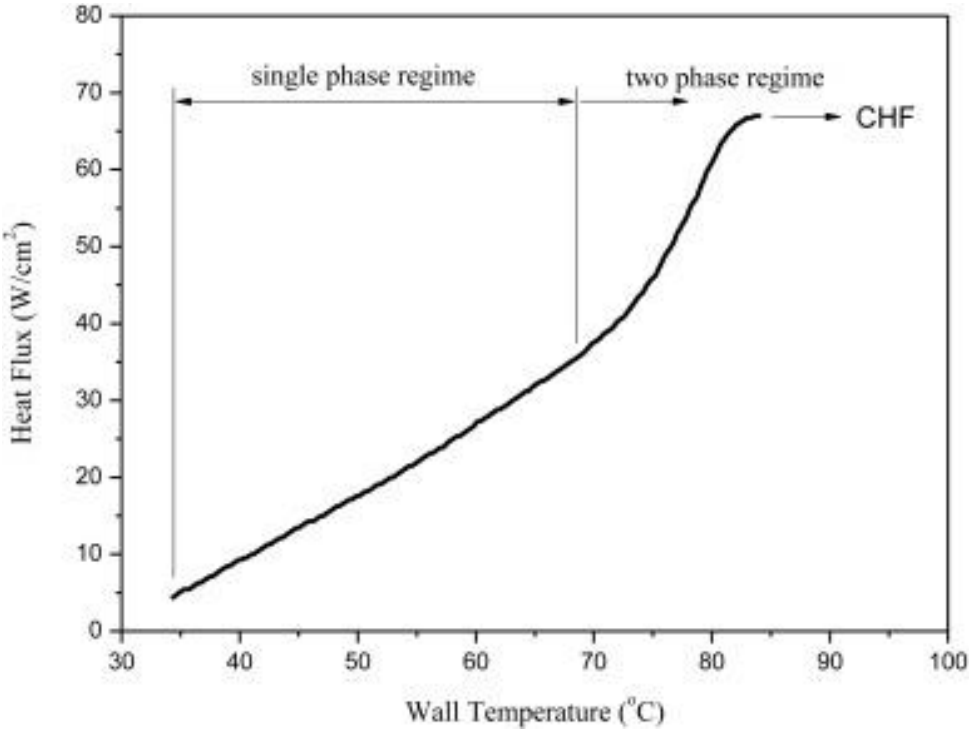

Fig. 2. Spray Cooling Curve (Figure adapted from reference [9] with permission)

Cooling in the single-phase regime is undoubtedly worse, but it is more stable due to no sudden changes in volume or pressure that can be caused by the water. Higher wall temperatures result in fluid property changes and can change the fluid to a gas state if high enough. High wall temperatures are also not desirable in many applications, such as electronics cooling where components cannot currently exceed 90ºC. The heat flux increases sharply as the wall temperature increase and the system approaches the two-phase regime. Critical Heat Flux (CHF) is achieved when the heat flux no longer increases with the wall temperature. Researchers have identified three distinct modes of spray cooling, which are determined by the wall temperature and spray mass flux. [10] The first case is referred to as the dry wall stare or spray evaporative cooling, where all of the incoming spray is vaporized on the surface, The second state is called the flooded state or the spray film cooling state, where the impinging spray forms a persistent film on the surface. The third state is called the Leidenfrost state, where "provide explanation, vapor bubbles form at the interface, insufficient contact between fluid and surface, required high wall temp". Rybicki was able to characterize the Nusselt number of single-phase regime of spray cooling as $Nu = 4.70\ Re^{0.61} Pr_f^{0.32}$ [11]. Previous work has focused on system level parameters, such as spray distance and spray flux, but has not delved into surface parameters such as roughness. In particular, Chen et al. found that the mass flux of the spray does not have a significant impact on the CHF [12], they also found that the CHF increased with increasing droplet flux and increasing droplet velocity . Droplet diameter however, had a negligible effect on the spray cooling performance. Mudawar reported that there is an optimal nozzle spacing distance, given the size of the heat exchanger and the spray angle. [13] A nozzle placed too close to the heat exchanger can lead to insufficient coverage, and a nozzle placed too far can lead to suboptimal usage of the spray stream.

The tubes and fins of the heat exchanger are be evenly coated with a thin layer of water when the spray is dispersed into the airflow. The heat transfer increases due to evaporation at the interface of the film and the heat exchanger surface, forced convection between the free-flowing air and the liquid film, and liquid film interaction with the water induced airstream. It has been shown that adding small amounts of liquid droplets to a cooling gas stream enhances the heat transfer rates on solid objects upon which the gas stream impinges on. [14] [15]. Wen-Jei et al. studied the heat transfer performance of both water and ethylene glycol sprays on automotive radiators [16]. They found an average increase in heat transfer performance of about 45% for Reynolds numbers between 500 and 1000. However, the heat transfer performance decreased as the Reynolds number increased. He found that spraying water and ethylene glycol resulted in the same performance gains, which contributed to the conclusion that the increase in heat transfer is dominated by the formation of the liquid film, rather than the evaporation. Ethylene glycol evaporates at 197ºC while water evaporates at 100ºC, and with a heat exchanger fluid temperature of 88ºC, indicates that evaporation plays a negligible role in the increase in heat transfer.

In this study, we will focus on performance benefits derived from switching to spray cooling for air cooling, with parameter focus on surface roughness, spray duty cycle, and ambient operating temperatures. We define spray cooling as pressurized liquid leaving a spray nozzle which results in a fine mist which impinges upon the heat exchanger downstream of the nozzle. In this work significant performance increases are found when switching from air cooling to spray cooling, and marginal performance decreases when switching from spray cooling to pulse spray cooling. This is specifically impactful in the alternative energy vehicle department as small tanks of water

can yield a greater than 100% increase in heat transfer performance across a wide range of conditions.

CHAPTER 2: Experimental Methods

2.1 Test Sample and Surface Coating Process

The heat exchangers utilized in this test were 3.25 in x 3 inches with a depth of 0.55 inches and 14 fins per inch. The internal tube diameter was 0.225 inches.

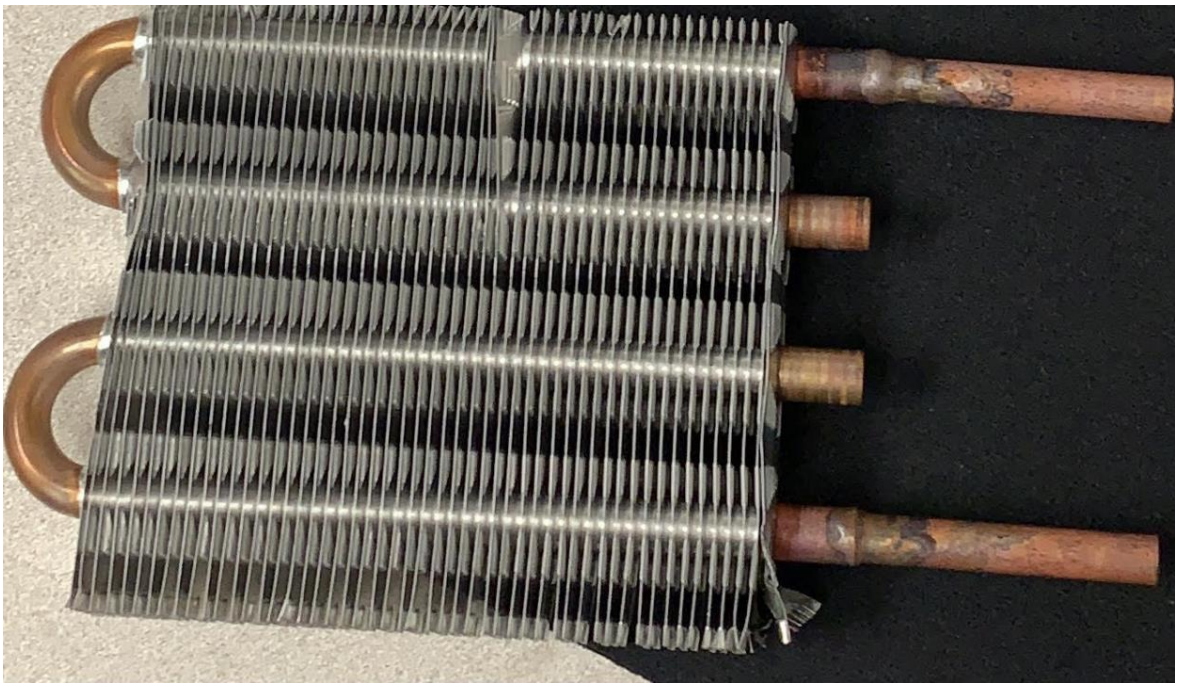

Fig. 3. Example heat exchanger

The untreated heat exchangers utilized in the experiments were hydrophilic by nature. Superhydrophilic heat exchangers were fabricated by first cleaning the as received heat exchanger with acetone, ethanol, and de-ionized water. Then, the heat exchangers were placed in 100°C de-ionized water for an hour to grow a uniform layer nanoscale boehmite (Aluminum Oxy-Hydroxide, Al(O)OH) structures (~50nm length scale, Fig. 5). This process results in a surface with nanoscale roughness features, which help promote hydrophilicity and enhance the wickability of the surface. The wettability of the superhydrophilic and unaltered heat exchanger

were characterized by measuring their apparent advancing contact angles (CA) (Table 1) on a micro goniometer.

Table 1: Surface wettability

Surface	Contact Angle	Hysteresis
Unaltered	106°	±19°
Superhydrophilic	5°	±1°

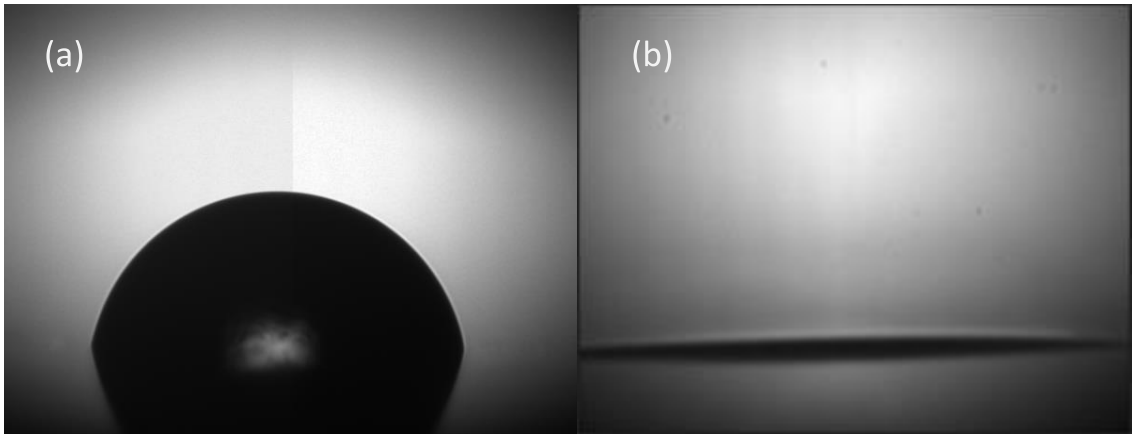

Fig. 4. Image of a droplet on the surface of the (a) uncoated heat exchanger , and (b)the superhydrophilic heat exchanger.

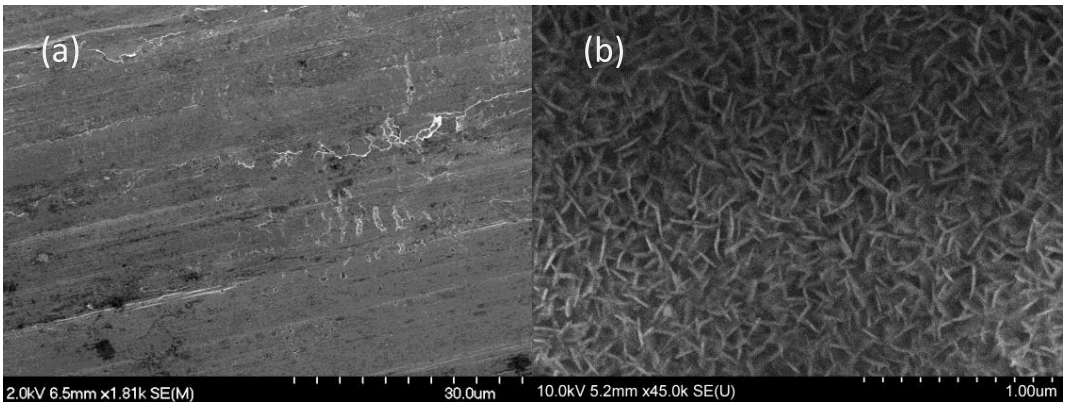

Fig. 5. Scanning electron microscopy images of (a) uncoated heat exchanger surface, (b) same surface after bohemetization resulting in a superhydrophilic surface.

2.2 Experimental Facility

The heat exchangers were tested in a closed-loop wind tunnel (Fig. 6) that was designed according to the specifications provided in ANSI/AHRI Standard 210/240-2008. The circular sections of the wind tunnel are 35.5 cm in diameter and made of insulated aluminum ducting to prevent parasitic temperature losses. A Polyscience AD15H heated recirculating bath provided hot fluid (50% Ethylene glycol-water solution) to the heat exchanger mounted in the wind tunnel test section. A flow straightener comprised of honeycomb Nomex material was placed in front of the test section to straighten the airflow and reduce swirling in front of the test section. A 2hp Dayton 4Z380A motor was used to precisely control the air velocity (v_{air}). The air velocity was calculated by measuring the pressure drop across a smooth converging nozzle (Inlet diameter =35.5cm, Outlet diameter = 12.7 cm), and then computed using equation (1).

$$v_{air} = \sqrt[2]{\frac{2\Delta P_{\text{nozzle}} A_2^2}{\rho_{\text{air}}(A_1^2 - A_2^2)}} \qquad (1)$$

The clear acrylic test section housing the heat exchangers has an inner cross-sectional area of 30.5cm x 20.5 cm. The test section featured inlet and outlet thermocouple grids to measure inlet and outlet air temperatures, and drilled mounting locations for stable, and repeatable placement of heat exchangers. The humidity of the wind tunnel was kept constant and controlled via a humidifier (PS-8.5 (s), Pure Humidifier Company), and a PID controller (Honeywell UDC3200). Likewise, temperature the air temperature was by a set of resistance coil heaters connected to a Watlow 982 PID controller. A pre-conditioning chiller loop was also added to the wind tunnel to cool the air exiting the hot test section and maintain steady air temperatures throughout the experiments. The cooling fluid for the cooling loop was provided by an air-cooled chiller (Thermo Scientific Merlin M150).

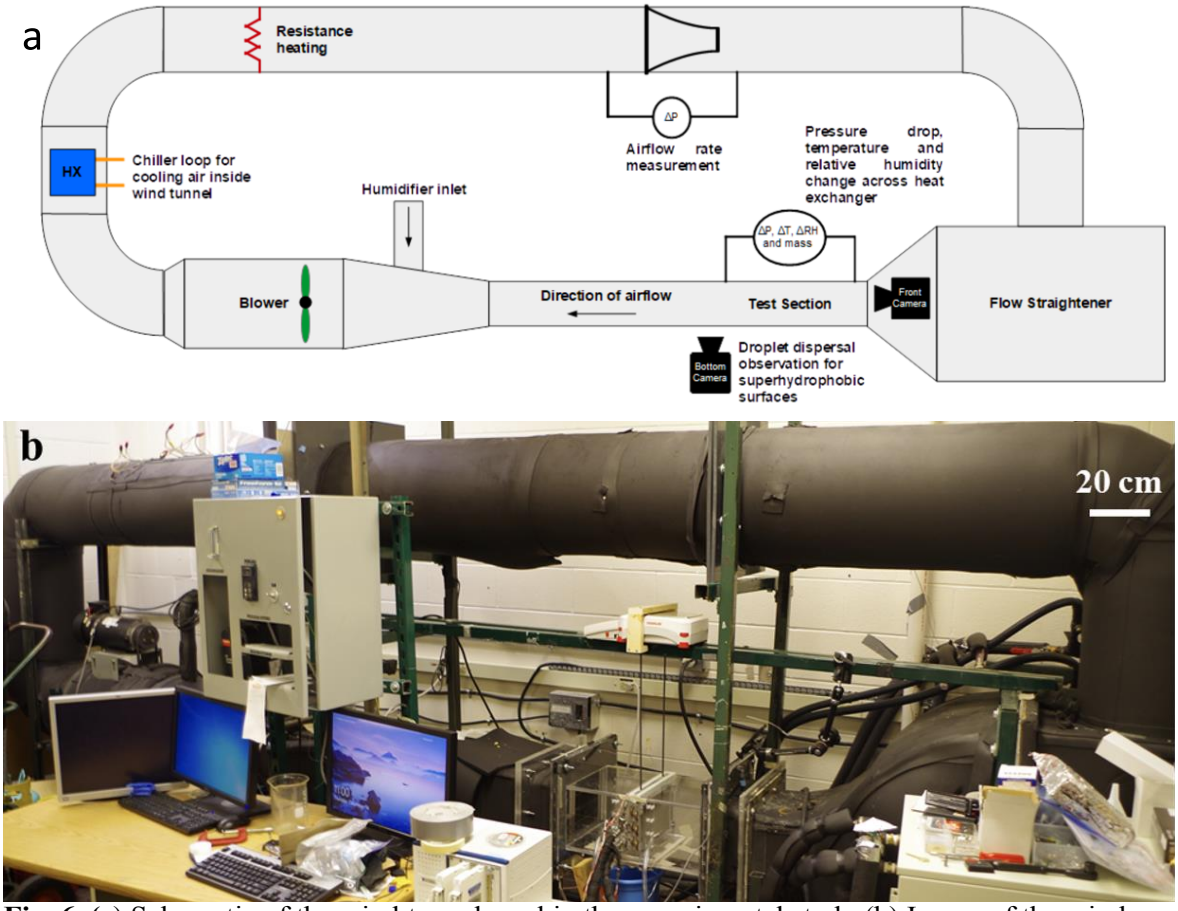

Fig. 6. (a) Schematic of the wind tunnel used in the experimental study (b) Image of the wind tunnel

A Seaflow 100PSI diaphragm pump powered the spray cooling setup nozzle. A spray nozzle with an orifice diameter of 0.01" was mounted onto a manifold that was connected to the pump. Cold and hot water for the spray nozzle was provided by a Polyscience AD15H bath. A pressure relief valve was added to the inlet of the pump to ensure that a constant 80 PSI was maintained in the manifold.

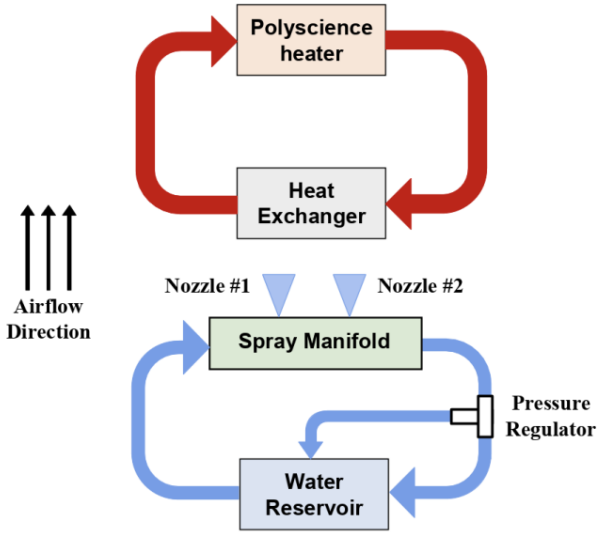

Fig. 7 Schematic of Spray cooling setup

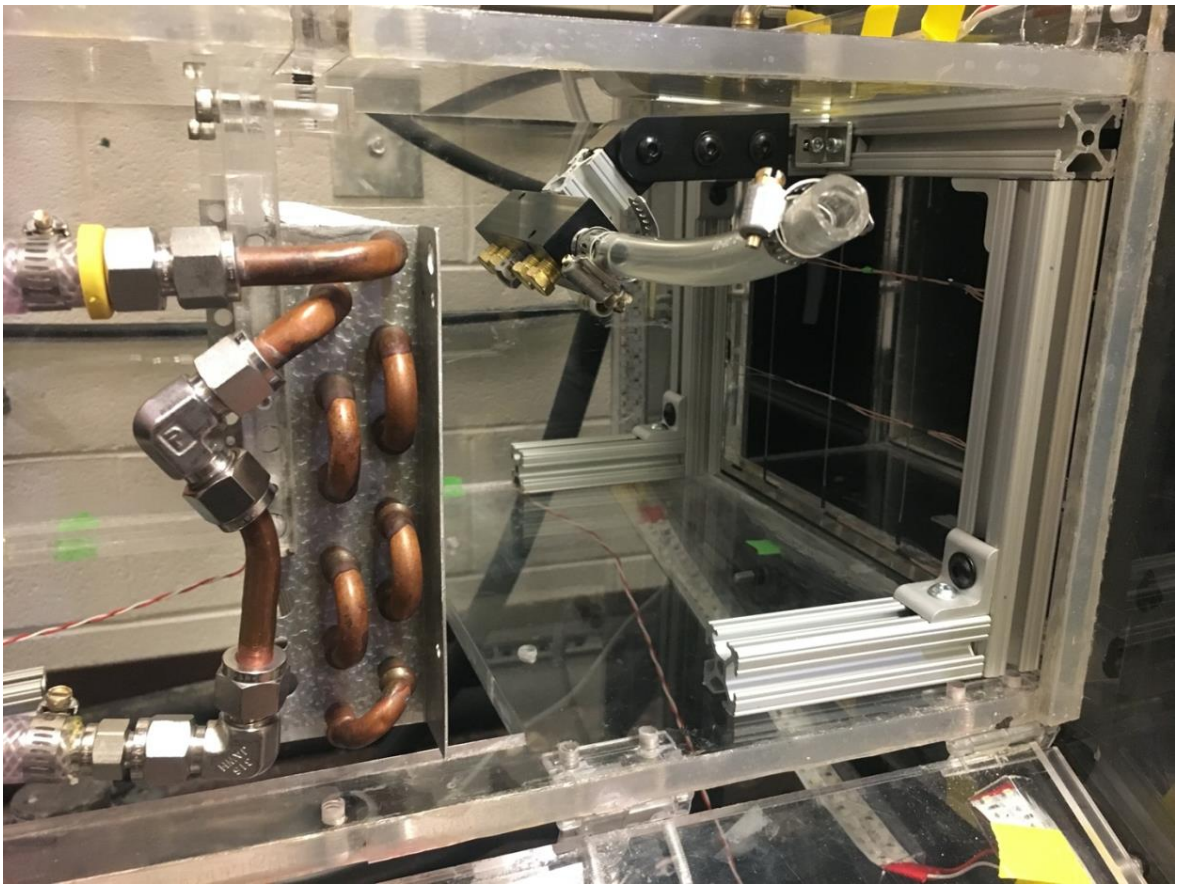

Fig. 8 Spray cooling setup

2.3 Instrumentation

Two thermocouple grids comprised of 20 K type thermocouples each (Omega, ±0.1°C) were used to measure the $T_{air,inlet}$ and $T_{air,outlet}$. $RH_{\text{air,inlet}}$ and $RH_{\text{air,outlet}}$ were measured using hygrometers (Omega HX94a, ±2.5%). Two RTDs (Reotemp Pt385-ClassB (Standard) 100ohm, ±0.12%) were utilized to measure the $T_{\text{TF,inlet}}$ and $T_{\text{TF,outlet}}$. A differential pressure transducer (Setra 239, ±0.14%) measured the pressure difference across the nozzle (ΔP_{nozzle}). The mass flow rate hot fluid in the test heat exchanger ($\dot{m}_{\text{TF}}$) was measured using a magnetic inductive flow meter (Kobold, ±0.8%).

Table 2: Details of instrumentation on test facility and the uncertainty for each measurement

Measurement	**Instrument**	**Span**	**Uncertainty**
Coolant Temperatures	RTD	-50 to 120°C	$\pm(0.0012T + 0.30°\text{C})$
Air Inlet Temperature	K-Type Thermocouple	0 to 100°C	±0.25°C
Coolant Flow Rate	Electromagnetic Flow Meter	0 to 40 L min^{-1}	$\pm(0.008\dot{V} + 0.12\ \text{L min}^{-1})$
Relative Humidity	Hygrometer	0 to 100%	±2.5%
Ambient Temperature	Hygrometer	-30 to 75°C	±0.6°C

2.4 Experimental Parameters and Calculations

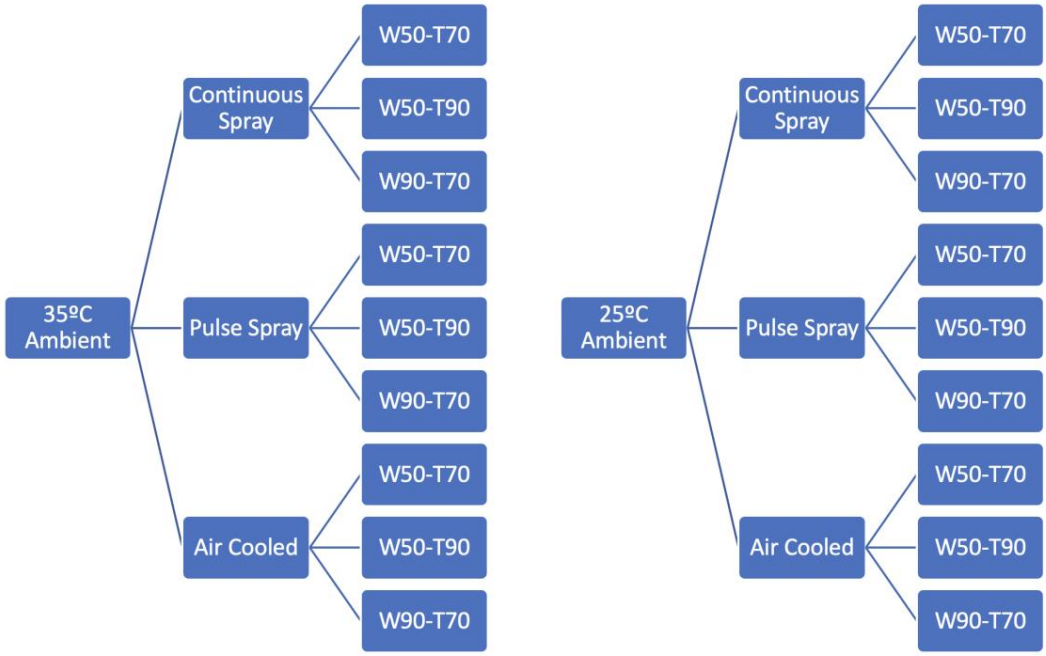

Fig. 9. Experimental Parameters

The performance of the heat exchangers was recorded under a variety of test conditions: ($T_{air,inlet}$ = 25°C & 35°C), (V_{air}= 70% & 100%), (T_{TF} = 70°C & 90°C), ($RH_{\text{air,inlet}}$ = 50%), (ST = 5°C& 60°C), (SP= 100PSI). The wind tunnel and heating baths were operated for an hour to stabilize the air, to fluid, and spray temperatures. The Thirty minutes of steady-state data was collected for each sample point after the air temperature had stabilized

CHAPTER 3: Results and Discussion

3.1 25°C $T_{air,inlet}$

Figure 10 is a typical plot of the heat transfer rate observed during an experiment. The average of the heat transfer rate was taken and condensed into bar graphs for easier analysis.

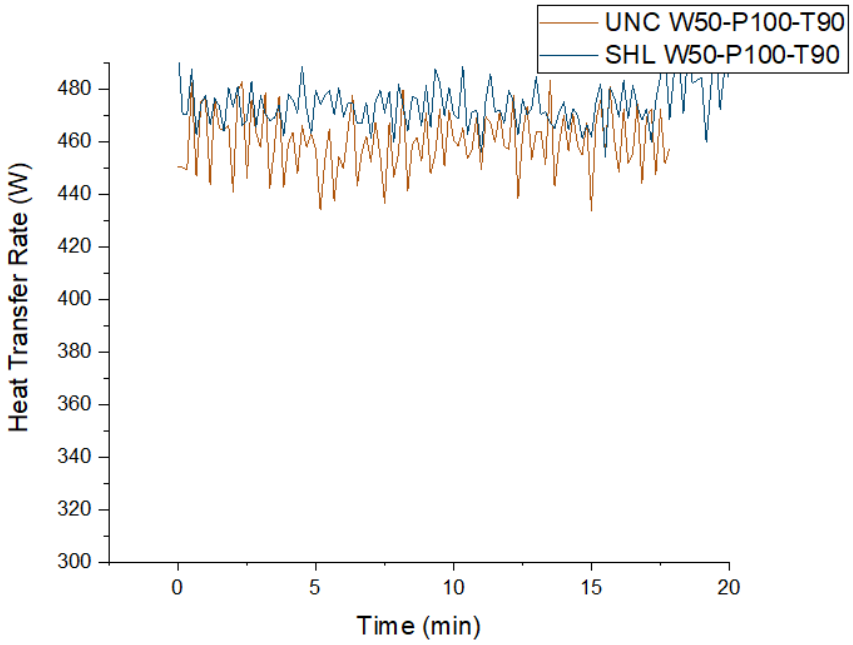

Fig. 10 Heat transfer rate over time of pulse cooling

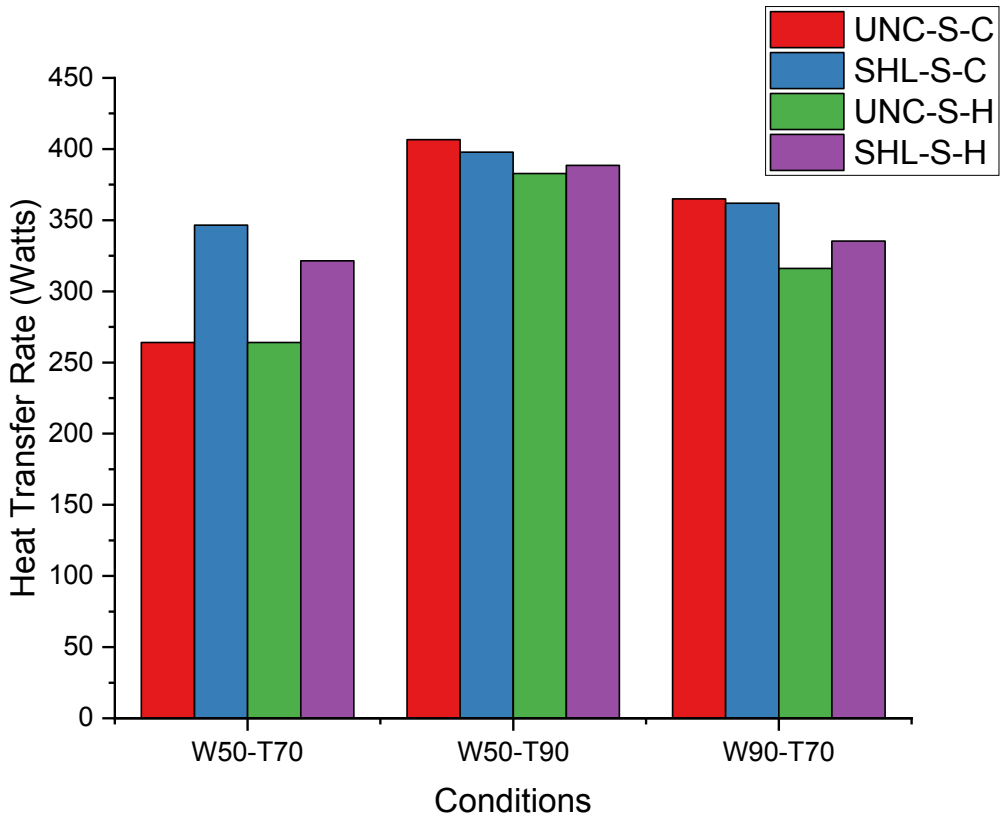

Fig. 11. Uncoated vs Superhydrophilic

Figure 11 shows the heat transfer rates of uncoated and superhydrophilic heat exchangers tested in 25°C air. Uncoated heat exchangers, and Superhydrophilic are labeled as UNC and SHL respectively. S is spray, P is pulse spray, C is cold temperature spray, and H is hot spray. W50 denotes a wind velocity of 2.0 m/s, and W90 denotes a wind velocity of 3.0 m/s. T70 denotes a fluid temperature of $70°C$ while T90 denotes a fluid temperature of $90°C$.All tests were ran at P100, which represents a pump flow rate of 1.3 L/min. Superhydrophilic heat exchangers outperform or match the uncoated heat exchangers in all the conditions, with the greatest difference in performance under lower fluid temperatures and lower windspeeds. In particular, superhydrophilic heat exchangers increase the heat transfer rate by an average of 9.6% across all the tests. As the wind speed increases; the heat transfer mechanism is dominated by thin film

spreading. Superhydrophilic surfaces naturally spread water, but as the wind speed increases, the wind will increase spreading on the uncoated surfaces, which causes their performance to converge with the superhydrophilic heat exchanger Additionally, the cold spray outperforms the hot by 6.5% on average, indicating that higher heat capacity leads to better performance in spray cooling.

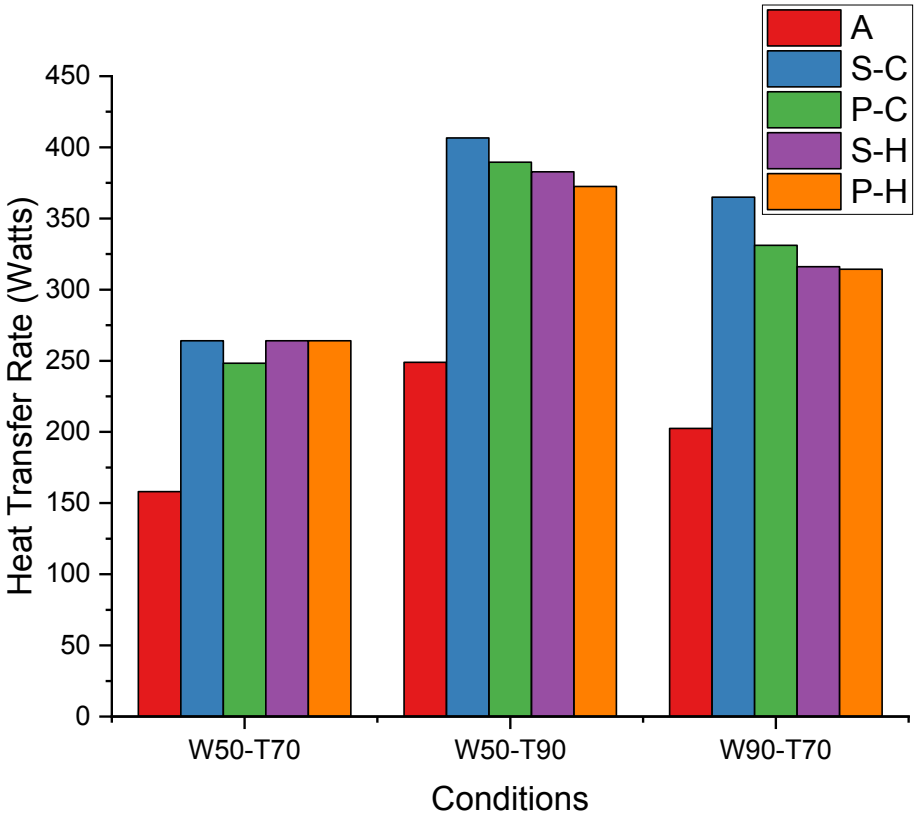

Fig. 12. Uncoated Comparison

In figure 12, A represents air cooled, i.e. no spray cooling, S represents spray, and P represents pulse spray (where the nozzle is turned on for 6 seconds, and off for 10 seconds, and the cycle is repeated for the duration of the test). When observing the uncoated results, spray cooling displayed on average a 64.5% increase in performance across the test cases. Cold spray displayed

a 70% increase while hot spray displayed a 59% increase in performance, indicating the additional ΔT from the cold spray improves performance significantly. Comparing continuous spray vs pulse spray experiments, there is only a 3.7% drop in performance on average. This is promising as it indicates that great performance benefits over air cooled can be achieved with only a small spray duty cycle and is something that should be investigated in the future for further optimization of the system.

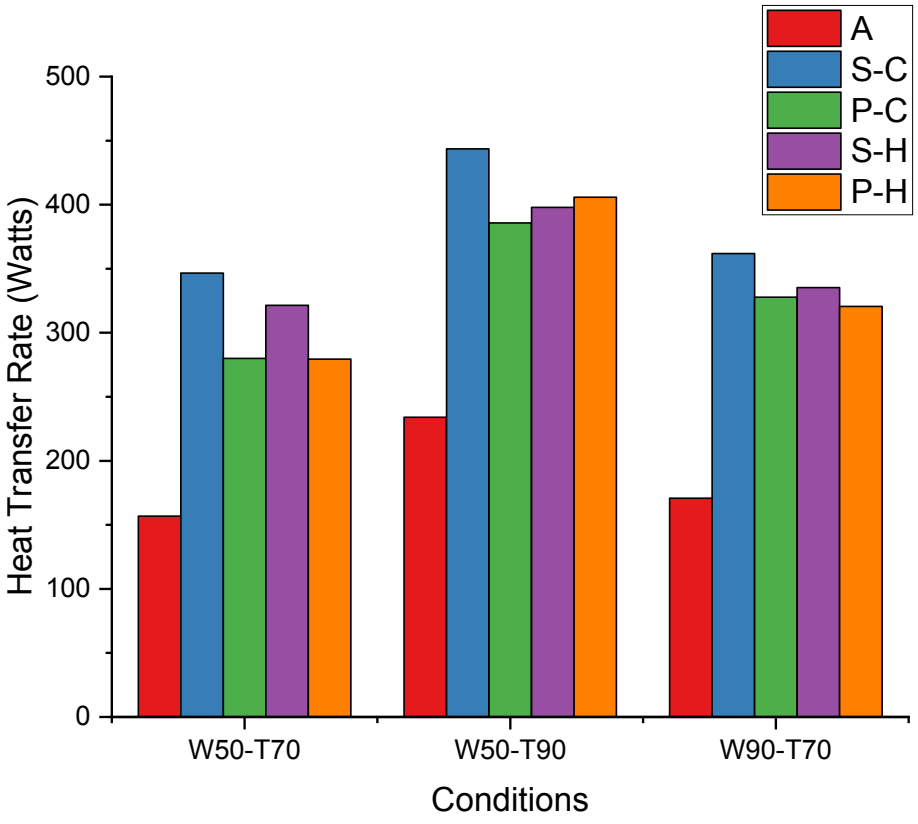

Fig. 13. Superhydrophilic Comparison

The superhydrophilic heat exchanges yield a 99% increase in performance when switching from air cooled to spray cooled. Cold spray displayed a 107% increase while hot spray displayed a 90.5% increase in performance, indicating again the additional ΔT from the cold spray improves performance significantly. Its interesting to note that the difference in the uncoated heat exchangers was 64.5%, indicating a great improvement of 34.5% when switching the surface roughness. However, when going from spray cooling to pulse spray cooling, we notice a 9.5% drop in performance, greater than the 3.7% drop seen in uncoated hx. This indicates that the superhydrophilic heat exchanges spread thin film water better than uncoated and will thus suffer more in peak performance when switching to pulse spray. However, it is important to note that the superhydrophilic heat exchangers still exhibit 4.6% better performance in pulse spray than uncoated ones.

3.2 35°C $T_{air,inlet}$

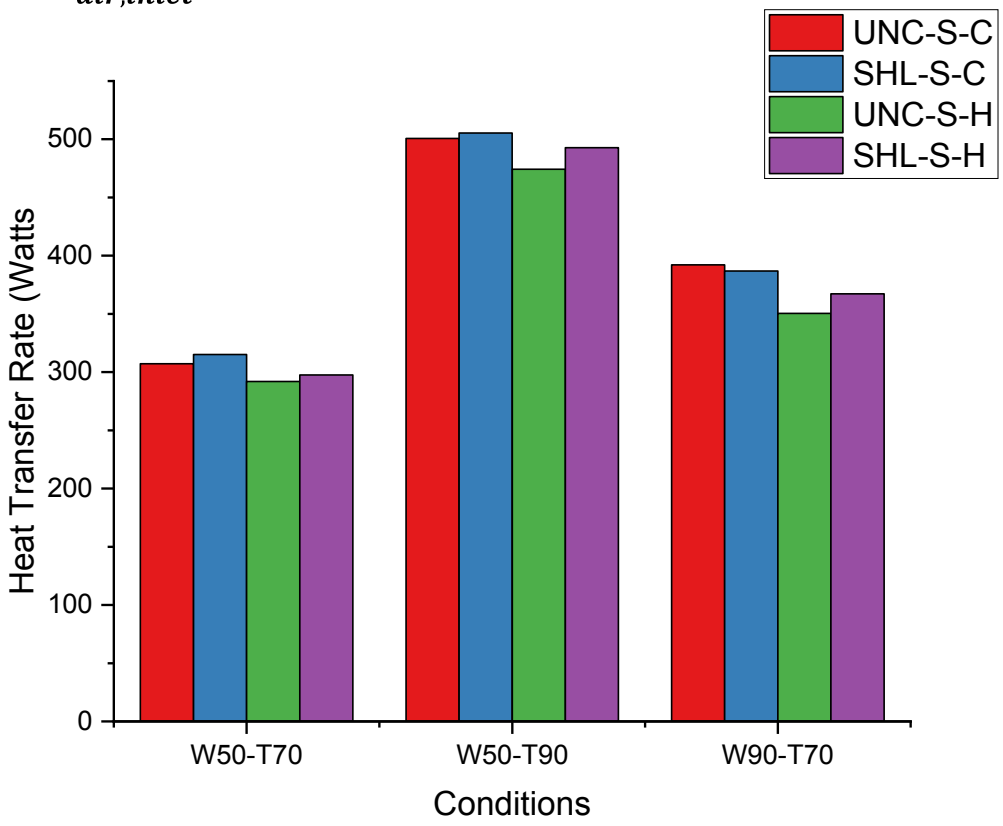

Fig. 14. Uncoated vs Superhydrophilic

In the higher ambient air conditions, superhydrophilic heat exchanges again outperform or match the uncoated heat exchangers in all of the test conditions, with the performance difference being relatively independent of temperature and wind speed. The superhydrophilic heat exchangers outperformed the uncoated ones on average by 2.1%, which while significant, is not as great of a performance boost seen in 25ºC ambient air, indicating lower ambient temperatures yield higher benefits when changing surface roughness. At higher temperatures the inherent evaporation rate is higher, which means more water will evaporate before completely spreading on the superhydrophilic surfaces, which is the reason uncoated and superhydrophilic surfaces perform

so closely at higher temperatures. Additionally, the cold spray outperforms the hot by 6% on average.

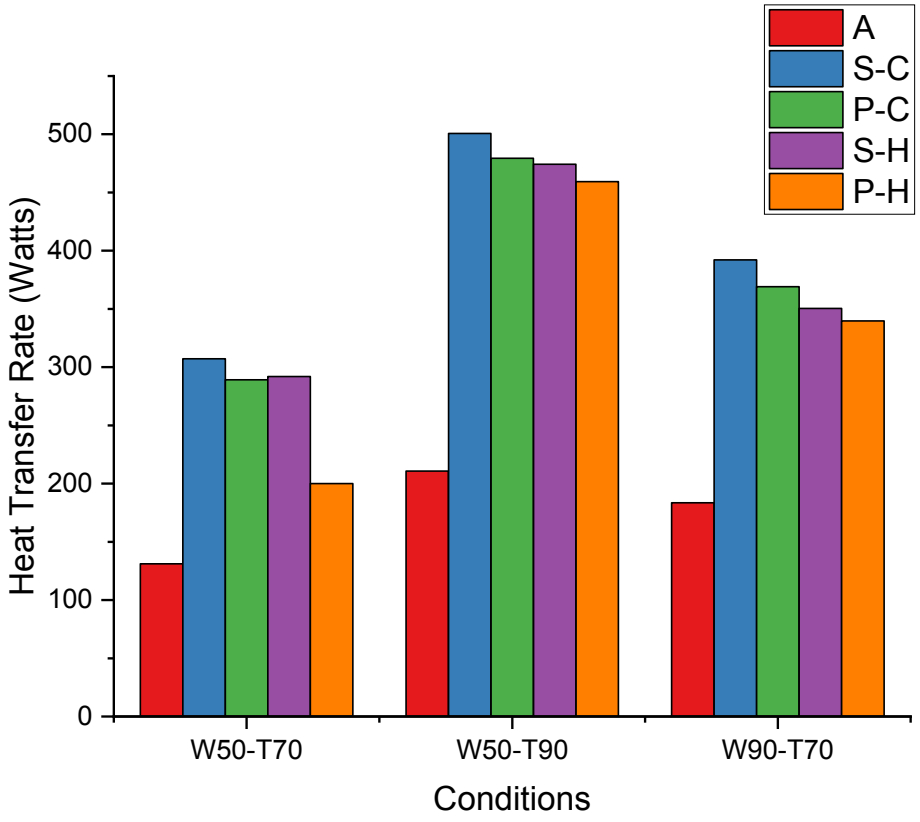

Fig. 15. Uncoated Comparison

The measured heat transfer rate in the air-cooled conditions was on average 175 watts, for the spray cooled it was 386 watts, a 120% increase in performance. This increase was almost double the 64.5% increase seen at 25ºC ambient temperature, indicating performance gains increase as ambient temperature increases. Cold spray displayed a 128% increase from air cooled while hot spray displayed a 112% increase in performance, indicating the additional ΔT from the cold

spray improves performance significantly. The measured heat transfer for continuous spray was on average 386 watts, 356 watts for pulse spray, showing an 8.4% drop in performance on average. The continuous spray still shows a 103% increase in performance over the air-cooled experiments, indicating promising results with even a small spray duty cycle.

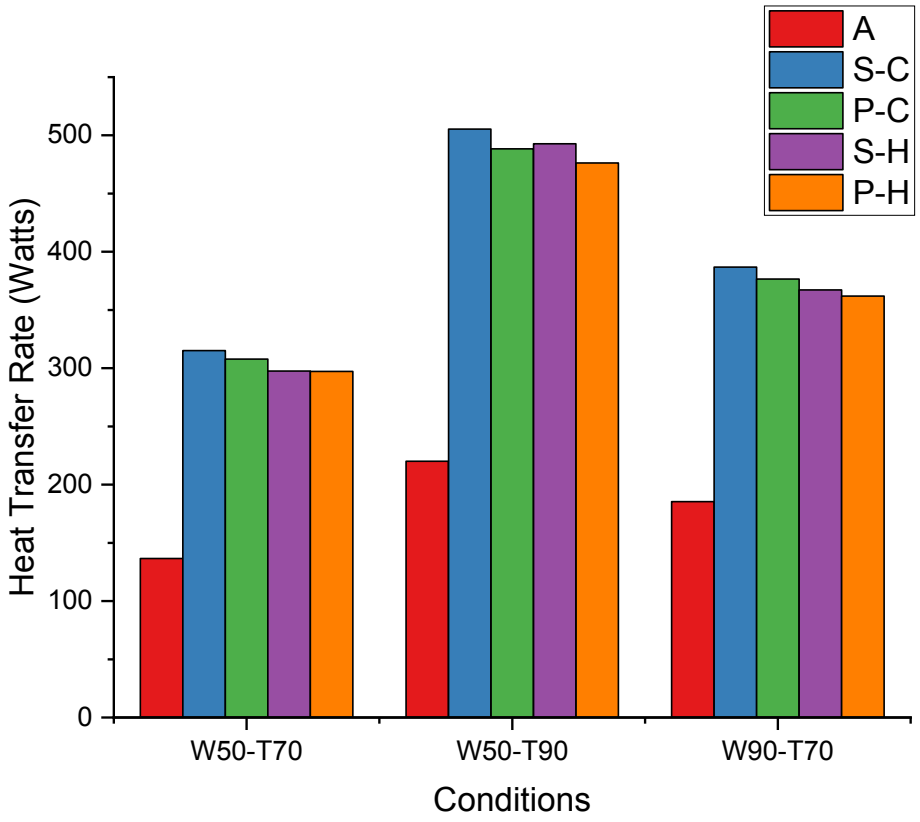

Fig. 16. Superhydrophilic Comparison

The superhydrophilic heat exchangers yield a 118% increase in performance at 35ºC when switching from air cooled to spray cooled. Cold spray displayed a 122% increase while hot spray displayed a 113% increase, indicating again the performance gains in ΔT of the spray liquid. The uncoated heat exchangers displayed a performance increase of 120%, indicating that switching

surface roughness at higher ambient temperatures does not increase performance, unlike in lower ambient temperatures. When moving from spray cooling to pulse spray cooling, a 2.45% decrease in performance is noted. This is again promising as the volume in liquid sprayed is drastically decreased while the performance marginally decreases.

CHAPTER 4: Conclusions

This study looked into the performance benefits of utilizing spray cooling in continuous and pulse form to enhance heat transfer for alternative energy vehicles. Spray cooling had been previously primarily studied and utilized in electronics cooling, but no experiments had been conducted on performance with surface roughness manipulation. A simple and scalable surface process was utilized to modify heat exchangers in this study. Results show that switching from air cooling to spray cooling can have up to a 128% increase in performance. The study found that at lower ambient temperatures, surface roughness has a profound effect in performance, while at higher temperatures the difference between uncoated and superhydrophobic heat exchangers is negligible. The study also found that the performance difference between air cooling and spray cooling is greater at higher temperatures, indicating great advantages in vehicles operating in hotter climates. Additionally, the difference in performance between pulse spray and continuous spray is less than 10% in all conditions, showing promise for automotive environments where space to store water is minimal.

This work focused on outlining the performance benefits between air cooling and spray cooling, with parameter variation focused on spray duty cycle, surface roughness, and ambient temperature. Further work should expand into lower and higher ambient temperatures for extreme cases, along with smaller duty cycles to build a performance benefit vs spray duty cycle. Additionally, higher wind velocities would be beneficial to ascertain the performance benefits of highway driving. This will help build a performance outline for greater vehicle scenarios.

References

[1] K. A. Estes and I. Mudawar, "Comparison of two-phase electronic cooling using free jets and sprays," *J. Electron. Packag. Trans. ASME*, vol. 117, no. 4, pp. 323–332, 1995, doi: 10.1115/1.2792112.

[2] K. Oliphant, B. W. Webb, and M. Q. McQuay, "An experimental comparison of liquid jet array and spray impingement cooling in the non-boiling regime," *Exp. Therm. Fluid Sci.*, vol. 18, no. 1, pp. 1–10, 1998, doi: 10.1016/S0894-1777(98)10013-4.

[3] T. A. Shedd, "Next Generation Spray Cooling: High Heat Flux Management in Compact Spaces," *Heat Transf. Eng.*, vol. 28, no. 2, pp. 87–92, Feb. 2007, doi: 10.1080/01457630601023245.

[4] A. C. Cotler, E. R. Brown, V. Dhir, and M. C. Shaw, "Chip-level spray cooling of an LD-MOSFET RF power Amplifier," *IEEE Trans. Components Packag. Technol.*, vol. 27, no. 2, pp. 411–416, Jun. 2004, doi: 10.1109/TCAPT.2004.828550.

[5] S. Chakraborty, I. Sarkar, A. Ashok, I. Sengupta, S. K. Pal, and S. Chakraborty, "Synthesis of Cu-Al LDH nanofluid and its application in spray cooling heat transfer of a hot steel plate," *Powder Technol.*, vol. 335, pp. 285–300, 2018, doi: 10.1016/j.powtec.2018.05.004.

[6] W. L. Cheng, W. W. Zhang, H. Chen, and L. Hu, "Spray cooling and flash evaporation cooling: The current development and application," *Renew. Sustain. Energy Rev.*, vol. 55, pp. 614–628, 2016, doi: 10.1016/j.rser.2015.11.014.

[7] T. Cader, L. J. Westra, and R. C. Eden, "Spray cooling thermal management for increased device reliability," *IEEE Transactions on Device and Materials Reliability*, vol. 4, no. 4. pp. 605–613, 2004, doi: 10.1109/TDMR.2004.838978.

[8] S. D. Sienski K, Eden R, "3D Electronic Interconnect Packaging.pdf," pp. 363–73, 1996.

[9] J. Kim, "Spray cooling heat transfer: The state of the art," *Int. J. Heat Fluid Flow*, vol. 28, no. 4, pp. 753–767, 2007, doi: 10.1016/j.ijheatfluidflow.2006.09.003.

[10] T. Tb, W. M. Grissom, and F. A. Wierum, "LIQUID SPRAY COOLING OF A HEATED SURFACE boy CP, 4 d," *Heour Mnn Transf.*, vol. 24, no. 866, pp. 261–271, 1981, [Online].

Available: https://ac.els-cdn.com/001793108190034X/1-s2.0-001793108190034X-main.pdf?_tid=cb89f407-cbd8-4d5c-b2d8-b7dd0c300b1b&acdnat=1536654494_5b5696cf32c17ec84c078378ab297b64.

[11] J. R. Rybicki and I. Mudawar, "Single-phase and two-phase cooling characteristics of upward-facing and downward-facing sprays," *Int. J. Heat Mass Transf.*, vol. 49, no. 1–2, pp. 5–16, 2006, doi: 10.1016/j.ijheatmasstransfer.2005.07.040.

[12] R. H. Chen, L. C. Chow, and J. E. Navedo, "Optimal spray characteristics in water spray cooling," *Int. J. Heat Mass Transf.*, vol. 47, no. 23, pp. 5095–5099, 2004, doi: 10.1016/j.ijheatmasstransfer.2004.05.033.

[13] I. Mudawar and K. A. Estes, "Optimizing and predicting CHF in spray cooling of a square surface," *J. Heat Transfer*, vol. 118, no. 3, pp. 672–679, 1996, doi: 10.1115/1.2822685.

[14] M. G. SCHERBERG, H. E. WRIGHT, and W. C. ELROD, "Heat-Transfer Potential of Liquid–Gas Spray Flows," *Proc. Int. Symp. Two-Phase Syst.*, pp. 739–752, 1972, doi: 10.1016/b978-0-08-017035-0.50044-6.

[15] S. D. Harris, "Spray Cooling of Heated Cylinders.," *AIChE Symp. Ser.*, vol. 74, no. 174, pp. 67–72, 1978.

[16] Y. Wen-Jei and D. W. Clark, "Spray cooling of air-cooled compact heat exchangers," *Int. J. Heat Mass Transf.*, vol. 18, no. 2, pp. 311–317, 1975, doi: 10.1016/0017-9310(75)90162-3.